CHAPTER 5

# Curvature-Induced Sorting of Bilayer Membrane Constituents and Formation of Membrane Rafts

Veronika Kralj-Iglič[1,*] and Peter Veranič[2]

[1]*Institute of Biophysics, Faculty of Medicine, University of Ljubljana, Lipičeva 2, SI-1000 Ljubljana, Slovenia and Laboratory of Physics, Faculty of Electrical Engineering, University of Ljubljana, Ljubljana, Slovenia*

[2]*Institute of Cell Biology, Faculty of Medicine, University of Ljubljana, Lipičeva 2, SI-1000 Ljubljana, Slovenia*

**Contents**



**Abstract**

The shape of a heterogeneous bilayer membrane, itself being formed of membrane constituents, and lateral and orientational distributions of constituents, are consistently related and act together to stabilize the configuration of the membrane. As constituents have different intrinsic shapes and properties they may energetically favor particular membrane curvature (e.g. curvature of spherical buds or tubular buds or narrow necks). Due to consequent accumulation of particular membrane constituents and due to direct interactions between them they would more likely coalesce into rafts and raft domains in specifically curved regions that can therefore be considered curvature specific to some extent. We call the above process that may lead to diverse functional units in the cell membrane a curvature-induced sorting of membrane constituents.

## 1. INTRODUCTION

The major improvement to the description of the cellular membrane by the fluid mosaic model [1] has been put forward by introducing lateral structural domains in the membrane. Within the upgraded fluid mosaic model the membrane is described as composed of constituents, that may be single molecules or their complexes. These complexes consist of just a few molecules (e.g. phospholipid–cholesterol complexes [2] or small protein–cholesterol–phospholipid

*Corresponding author. Tel: +386-41-720766; Fax: +386-1-4768850;
E-mail: veronika.kralj-iglic@fe.uni-lj.si

ADVANCES IN PLANAR LIPID BILAYERS AND LIPOSOMES, VOLUME 5
ISSN 1554-4516 DOI: 10.1016/S1554-4516(06)05005-8

complexes), or they may coalesce into larger domains (e.g. rafts, raft domains and calveolae) [3–6].

The lateral membrane heterogeneity in terms of co-existing lateral lipid domains with different molecular composition and distinct physical properties has been intensively studied in biological membranes [3,7–13]. One of the aspects that regards mechanisms of formation of these domains is the local membrane curvature. As the membrane constituents are more or less free to move laterally over the membrane surface, they would accumulate in regions of energetically favorable local curvature while regions of unfavorable curvature would be depleted of these constituents. At regions of higher lateral density the direct interactions between constituents may promote separation into coexisting domains with a distinct composition and curvature. A particular membrane curvature within a structural domain can be considered its characteristic and is closely related to the function and configuration of the included protein molecules.

Structural domains were found in spherical regions of the buds in cells [11,13,14–19] while related processes have been observed also in multicomponent bilayer vesicles [11,15,17,19,20]. In biological cells, budding represents the first step in formation of small vesicles which are involved in transport of molecules through cell membrane and between cell organelles [5]. Analogously, the observed curvature-dependent domain formation in bilayer vesicles may result in fission of vesicles at domain boundaries [11,13,18,21]. In some cases, tubular shape of the membrane is preferred. Thin tubular membrane protrusions with specific composition of the membrane may be stable also without the inner supporting rod-like cytoskeleton [22]. For example, it was found that at subcellular level (irrespective of the cell type), the membrane protein prominin is preferentially localized in microvilli and other plasma membrane protrusions [7,10]. The so-called Lubrol rafts containing prominin were found to be distinct from the cholesterol–sphingolipid (Triton resistent) rafts in the planar parts of the membrane [10]. Further, the budding process involves narrowing of the neck connecting the daughter vesicle and the mother membrane. In the neck, there is a large difference between the two principal membrane curvatures i.e. the curvature is anisotropic. Therefore, the neck would be favored by specific membrane constituents that become orientationally ordered in the neck [23,24].

Besides the intrinsic properties of the molecules that constitute the structural domain, its membrane curvature and the corresponding lateral composition are determined by nonlocal effects that derive from maximization of entropy, constraints upon the membrane area and enclosed volume and interaction of each membrane leaflet with the surrounding solution. The nonlocal effects may drive the membrane to a point where budding would more likely to take place [19,20,23,25–27]. The above mechanisms may therefore result in curvature sorting of membrane constituents [13].

The scope of this contribution is accumulation of rafts on regions of specific curvature. We show experimental evidence on stable membrane structures of

particular shape in connection with membrane composition and present a corresponding theoretical description that is based on curvature sorting of the membrane constituents and direct interaction between constituents.

## 2. STABILITY OF TUBULAR MEMBRANE PROTRUSIONS

We consider a system where a tubular protrusion is formed due to some impact, such as formation of a rod-like structure near the inner cell surface (Fig. 1). The membrane constituents would then distribute over the membrane in such way as to minimize their free energy. Further, the membrane constituents may undergo orientational ordering in the plane of the membrane in those regions of the membrane that have a nonzero difference between the two principal membrane curvatures, which further decreases their membrane free energy. Stable structure is therefore described by the lateral and orientational distribution of membrane constituents which corresponds to the minimum of their free energy.

For simplicity we assume that the membrane is composed of two species of constituents (molecules or small complexes of molecules). One of the species is much less abundant than the other, however, due to its strong interaction with the

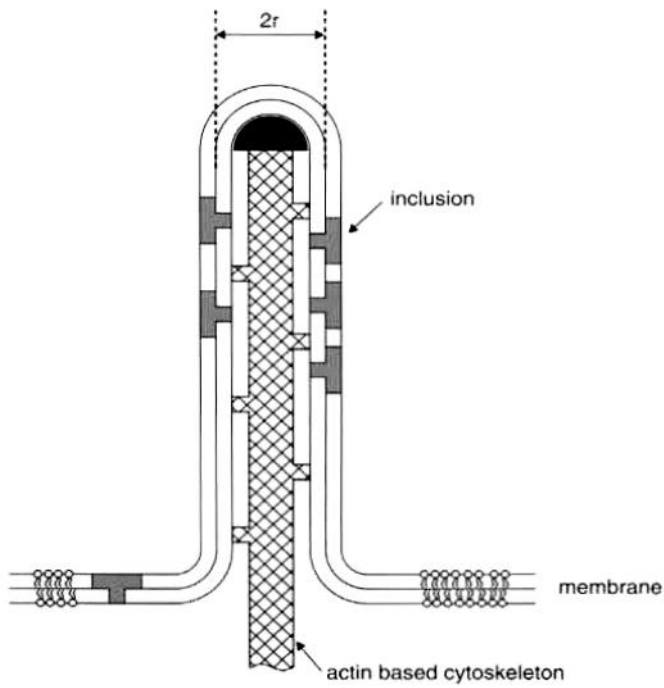


**Fig. 1.** Schematic illustration of curvature-induced accumulation of rafts in tubular membrane protrusions (adapted from Ref. [32]).

local membrane curvature, this species determines the free energy. We call these constituents the membrane inclusions. We assume that inclusions are intercalated into the membrane from one side only.

The membrane shape that would completely fit the inclusion is referred to as the shape intrinsic to the inclusion. The corresponding principal curvatures are denoted by $C_{1m}$ and $C_{2m}$ [23,28,29]. A schematic presentation of examples of small anisotropic inclusions is given in Fig. 2. In general, the local membrane shape differs from the intrinsic shape of the inclusion. This means that the principal curvatures of the actual shape differ from the principal curvatures of the intrinsic shape. The corresponding single-inclusion energy due to curvature mismatch is defined as the energy that is spent in adjusting the inclusion into the membrane and is determined by terms composed of two invariants of the mismatch tensor [30]. Terms up to the second order in the curvature tensor elements are taken into account. Upon statistical averaging over all possible orientations of the inclusion the free energy of the single inclusion can be written in the form [23,31]:

$$E_i = \frac{\xi}{2}(H - H_m)^2 + \frac{\xi + \xi^*}{4}\left(D^2 + D_m^2\right) - kT \ln\left(I_0\left(\frac{(\xi + \xi^*) D_m D}{2kT}\right)\right), \qquad (1)$$

where $\xi$ and $\xi^*$ are the interaction constants, $H = (C_1 + C_2)/2$ the mean curvature of the membrane, $H_m = (C_{1m} + C_{2m})/2$ the intrinsic mean curvature of the inclu-

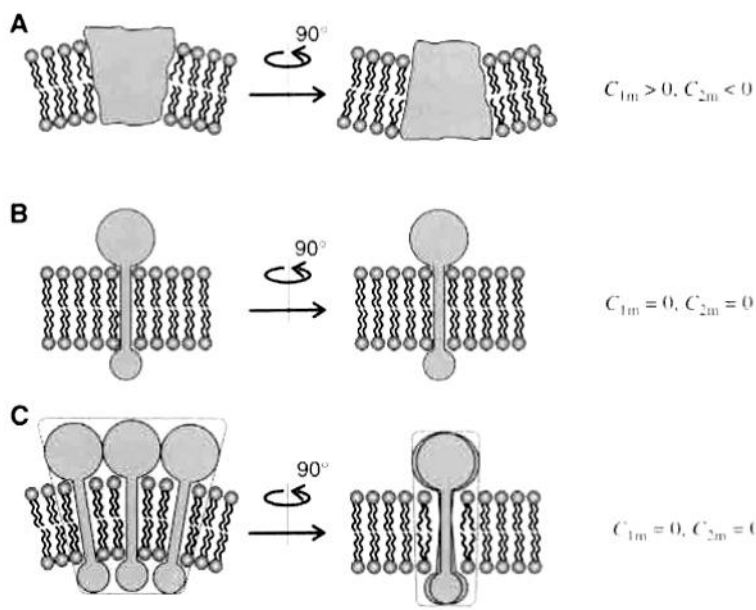


**Fig. 2.** Schematic illustration of different intrinsic shapes of membrane proteins (A,B) and of a membrane protein–lipid inclusion (C). The inclusion can have intrinsic curvatures $C_{1m}$ and $C_{2m}$ that in general differ from the intrinsic curvatures of the molecules which compose the inclusion (adapted from Ref. [13], see also [12]).

sion, $D = |C_1 - C_2|/2$ the membrane curvature deviator and $D_m = |C_{1m} - C_{2m}|/2$ the intrinsic curvature deviator of the inclusion, $C_1$ and $C_2$ the principal membrane curvatures, $kT$ the thermal energy and $I_0$ the modified Bessel function.

The free energy of inclusions is determined by the energies of inclusions and their collective effects. A lattice is imagined where some of the sites are occupied by equal and indistinguishable inclusions. Direct interactions between inclusions are taken into account. The free energy of inclusions per site ($f_i = F_i/(A/a_0)$) is [32]

$$f_i = kT \int n \ln n \, da + kT \int (1-n) \ln(1-n) \, da + \\ + \frac{cw}{2} \int n^2 \, da + \int n E_i \, da, \tag{2}$$

where $n$ is the fraction of the membrane area covered by inclusions at a given position $\mathbf{r}$, $A$ the membrane area, $a_0$ the area per inclusion, $w$ the energy of the nearest-neighbor interaction between inclusions [33,34], $c$ the number of the nearest neighbors, and $da$ the element of the normalized (relative) membrane area. The integration is performed over the entire (normalized) area of the membrane surface ($\int da = 1$). The first two terms in equation (2) represent the configurational entropy [33,34] while the third term describes the nearest-neighbor interaction energy between inclusions in the Bragg–Williams approximation [33,34].

The fraction of the membrane area covered by inclusions $n$ varies over the membrane surface as a function of the membrane curvature. By taking into account the conservation equation for all inclusions in the membrane: $\int n \, da = \bar{n}$ where $\bar{n}$ is the average value of $n$, a functional is constructed [32]:

$$\int (f_i + \lambda n) \, da = \int L(n) \, da, \tag{3}$$

where $\lambda$ is the Lagrange parameter. The variation is performed by solving the corresponding Euler equation $\partial L/\partial n = 0$ which gives the expression for the function $n$ [32]

$$n = \frac{\vartheta \exp(-E_i/kT)}{1 + \vartheta \exp(-E_i/kT)} \left[ 1 - \frac{4w}{kT} \frac{\vartheta \exp(-E_i/kT)}{(1 + \vartheta \exp(-E_i/kT))^2} \right], \tag{4}$$

where $\vartheta = \exp(-\lambda)$. In the above expression the nonlinear terms in $w$ are neglected. We took $c = 4$ for a square lattice [33]. For attractive nearest-neighbor interactions the parameter $w$ is negative $w < 0$. The parameter $\vartheta$ is determined from the condition $\int n \, da = \bar{n}$.

Since in the case considered the protrusion is formed due to the impact of the rod-like cytoskeletal structure, the shape of the membrane is fixed. For simplicity we consider that it is composed of two parts, a flat part with curvatures $H_f = D_f = 0$, and relative area $a_f$ and fraction of the area covered by the inclusions $n_f$, and a highly curved tubular part of the membrane with curvatures $H_t = D_t = 1/2r$ (where $r$ is the radius of tubular protrusions), relative area $a_t$ and fraction of the area covered

by inclusions $n_t$. The parameter $\vartheta$ is determined numerically from the condition

$$n_f a_f + n_t a_t = \bar{n}, \tag{5}$$

where we take into account that $a_f + a_t = 1$ while $n_f$ and $n_t$ are obtained by using equation (4).

Figure 3 shows the fraction of the area of the tubular membrane protrusions covered by anisotropic inclusions $n_t$ as a function of the radius $r$ for three values of the intrinsic curvature deviator of the inclusions $D_m$.

It can be seen that for small $r$ and large $D_m$ the fraction of the membrane area occupied by inclusions ($n_t$) is much larger than $\bar{n}$, while ($n_f$) is smaller than $\bar{n}$. This indicates a possibility of the curvature-induced accumulation of the membrane inclusions in highly curved tubular membrane regions. Because of high concentration in the tubular protrusion the inclusions may coalesce into rafts and raft domains. It can also be seen in Fig. (3) that for high enough values of the intrinsic curvature deviator of the inclusions $D_m$, the value of $n_t$ approaches unity indicating a possibility of the lateral phase separation of inclusions.

Our theoretical model provides an explanation for the observed curvature induced enrichment of raft markers in tubular membrane protrusions. Accumulation of inclusions on tubular protrusion and their orientational ordering lower the membrane free energy and therefore stabilize the tubular structure. It is therefore expected that the tubular shape of the protrusion is stable even without the inner rod-like structure [22]. This was confirmed in an experiment where the inner rod-like structures of tubular protrusions of the cell membrane were disintegrated. Membrane of the protrusions retained its tubular shape as described below.

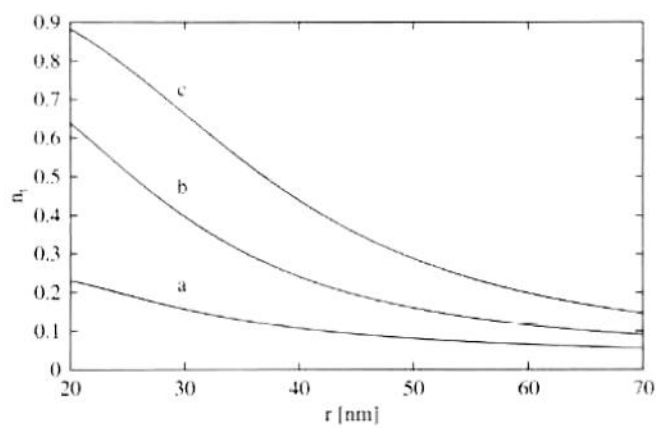


**Fig. 3.** The fraction of the area of a tubular membrane protrusion covered by anisotropic inclusions ($n_t$) as a function of the radius of the tube $r = 1/C_1$ for three values of the intrinsic curvature deviator of inclusions $H_m = D_m$: $0.03\,\mathrm{nm}^{-1}$ (a), $0.04\,\mathrm{nm}^{-1}$ (b) and $0.05\,\mathrm{nm}^{-1}$ (c). The values of the other model parameters are: $\bar{n} = 0.02$, $a_f = 0.02$, $w/kT = -0.12$ and $\xi = \xi^* = 5000\,\mathrm{kT\,nm}^2$ (adapted from Ref. [32]).

Cytochalasin B is a substance that disintegrates actin filaments of the cell cytoskeleton. Consequently, microtubules segregate into rod-like structures that exert an impact on the cell membrane. Fibroblasts treated with cytochalasin B for 30-min exhibit long flattened protrusions on a globular cell body, which are attached to the ground (Fig. 4(1A)). Inside such protrusion, a parallel array of microtubules can be seen in Fig. 4(1B). In cytochalasin B-treated cells with reduced content of cholesterol in the membrane (due to growth in a medium without cholesterol for 24 h) the protrusions are much thinner (Fig. 4(2A)), while no rod-like structures of microtubules could be found within the protrusions (Fig. 4(2B)). Further, no microspikes could be found on the protrusions

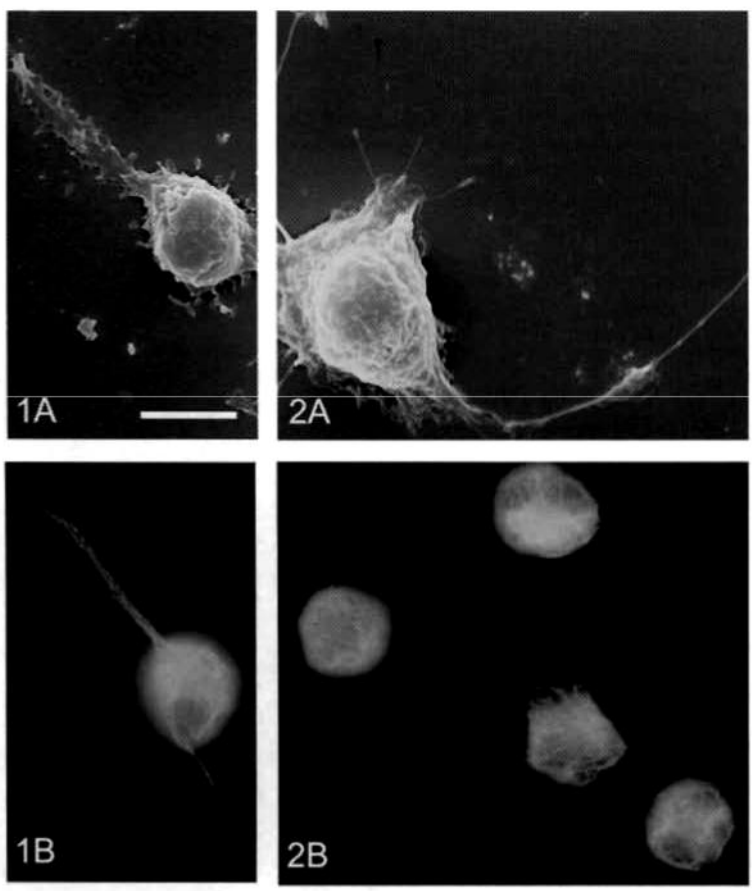


**Fig. 4.** In cells treated with cytochalasin B, long flattened membrane protrusions on globular cell bodies were found attached to the ground (1A). Immunofluorescence labeling of tubulin showed parallel rod-like organization of microtubules in these membrane protrusions (1B). Cytochalasin treatment of cells with mild cholesterol depletion resulted in thinner and more smooth tubular membrane protrusions (2A) where the rod-like microtubular structure completely disappeared (2B). Bar = 10 μm (adapted from Ref. [32]).

(Fig. 4(2A)) in contrast to the case shown in Fig. 4(1A). In cholesterol-depleted cells microtubules are concentrated only in the globular bodies of the cells close to the nuclei (Fig. 4(2B)). These experiments present evidence on tubular shapes that are stable also without the inner rod-like structures. Although the rod-like protrusions were formed due to the impact of the inner rod-like structure, the tubular shape was stable after the disintegration of the inner structure which is in agreement with the theoretical predictions.

It was shown that within the standard isotropic membrane elasticity models the stability of tubular membrane protrusions cannot be explained without an inner supporting rod-like structure or pulling mechanical force [35–37]. However, thin tubular membrane protrusions were found to be stabilized by anisotropic membrane components [22]. We suggest that the observed stability of thin tubular membrane protrusions without the inner supporting rod-like cytoskeleton (Fig. 4(2B)) may be a consequence of accumulation of anisotropic membrane components in the bilayer membrane of these protrusions.

Lubrol rafts are considered to be a novel type of membrane rafts (microdomains) that were found in tubular-shaped membrane regions and are distinct from the cholesterol–sphingolipid (Triton resistant) rafts that were found in the planar parts of the membrane [38]. In the presented theoretical consideration the applied value for the interaction constant $\xi$ was chosen to describe a small protein–lipid complex [39] and could therefore well describe the prominin–lipid complex. Small anisotropic protein–lipid complexes (i.e. anisotropic membrane inclusions) may associate into larger two-dimensional aggregates (Lubrol rafts) upon their curvature-induced accumulation in tubular protrusions as previously observed [5,10,32]. Our theoretical model therefore provides an explanation for the observed curvature-induced enrichment of Lubrol raft markers in tubular membrane protrusions.

The observed stability of thin tubular membrane protrusions without the inner supporting rod-like skeleton (Fig. 4) is in line with the assumption that prominin inclusions (and other strongly anisotropic membrane inclusions) have an important role in generation and stabilization of plasma membrane protrusions [10,22]. However, also in cases where there is a rod-like structure inside the tubular protrusion [37,40], the described accumulation of anisotropic membrane inclusions in tubular membrane protrusions, represents a complementary physical mechanism for stabilization of tubular membrane protrusions [20,22,30,41].

## 3. STABILITY OF SPHERICAL BUD AND NECK

A stable structure of unsupported membrane is described by the membrane shape and lateral and orientational distribution of membrane constituents that correspond to the minimum of the membrane free energy.

Spherical budding has been simulated by generating a sequence of shapes where a patch of the membrane due to increasing average mean curvature

develops a neck which undergoes thinning until a limit shape involving a small spherical bud connected to the almost flat part by infinitesimal neck is formed [39]. We assume that the membrane is composed of two species: inclusions that favor strongly curved isotropic curvature ($H_{m,i}$ is large and positive while $D_{m,i} = 0$), and isotropic components of the phospholipid moiety that favor flat regions ($H_{m,0} = D_{m,0} = 0$). The membrane free energy is composed from contributions of both species, $f = f_i + f_0$, where $f_i$ pertains to the inclusions and $f_0$ to the phospholipid moiety. Both contributions to the free energy are obtained by using equation (1) and the intrinsic parameters $H_{m,j}$, $D_{m,j}$ and $\xi_j = \xi_j^*$ ($j = i,0$) that correspond to the membrane constituents [21]. For each shape in the sequence, the membrane free energy is minimized with respect to the distribution of inclusions.

Figure 5 shows accumulation of the membrane constituents that favor high isotropic curvature on the small bud. The fraction of the area covered by inclusions increases toward the tip of the bud. As the neck becomes narrower, the distribution approaches a step function while the free energy of inclusions lowers the membrane free energy. The proposed mechanism is therefore relevant also for formation and stabilization of highly curved spherical membrane shapes with high concentrations of certain membrane constituents [16]. Figure 6 shows an example of intensive budding of vesicles in animal cells. The "*trans*" side of the Golgi apparatus is namely the origin of daughter vesicles which are directed to the plasma membrane or to lysosomes.

The properties of the neck-shaped regions are conveniently studied on undulated tubular shape. A parametric model can be used to generate such shape. It is assumed that the shape is obtained by rotating the function [21]

$$r(z) = R_0 + u \cdot \sin(qz), \tag{6}$$

around the $z$ axis. Here $r$ is the radial coordinate, $z$ the coordinate along the longitudinal axis, $R_0$ the average radius, $q$ the wave number of the modulation and $u$ its amplitude. From the constraint for the surface area per unit length (along

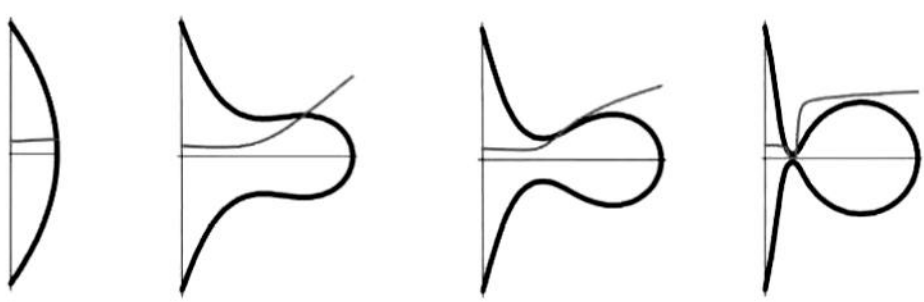

**Fig. 5.** The fraction of the membrane area covered by isotropic inclusions characterized by positive $H_{m,i}$, $D_{m,i} = 0$ and negative $w$ during the budding/vesiculation of the membrane and the corresponding shape of the bud (adapted from Ref. [13]).

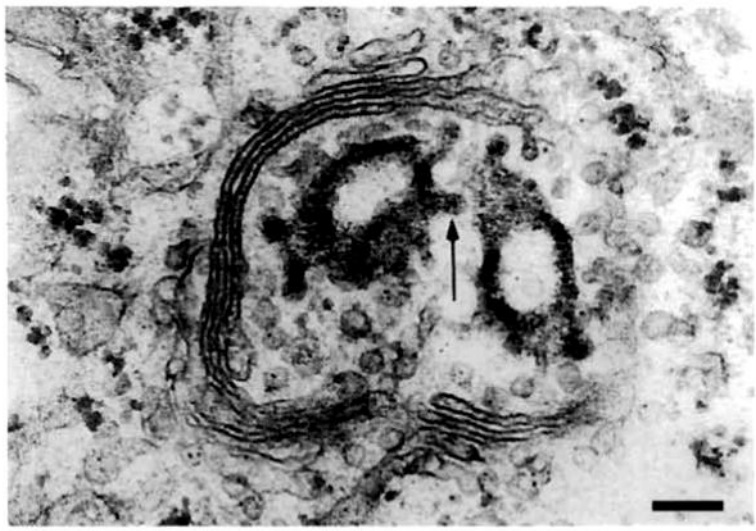

**Fig. 6.** The budding daughter vesicles (arrow) are frequently seen on trans cisternae of Golgi apparatus. Bar = 200 nm.

the $z$-axis) the parameter $R_0$ can be expressed as a function of $q$ and $u$ [21]

$$R_0 = \frac{A - 2\pi u \int_0^l \sin qz \sqrt{1 + u^2 q^2 \cos^2 qz}\, dz}{2\pi u \int_0^l \sin qz \sqrt{1 + u^2 q^2 \cos^2 qz}\, dz}, \tag{7}$$

where $l$ is the length of the segment. The expression (6) defines the mean and the Gaussian curvatures [21],

$$H = -\frac{1 + u^2 q^2 + R_0 u q^2 \sin qz}{2(R_0 + u \sin qz)(1 + u^2 q^2 \cos^2 qz)^{3/2}}, \tag{8}$$

and [21]

$$C_1 C_2 = -\frac{u q^2 \sin qz}{(R_0 + u \sin qz)(1 + u^2 q^2 \cos^2 qz)^2}, \tag{9}$$

while the curvature deviator is obtained by using the connection $D = \sqrt{H^2 - C_1 C_2}$.

Again, we assume that the membrane is composed of two species: inclusions and components of the phospholipid moiety, however in this case inclusions are assumed anisotropic so that they favor a saddle-like shape with $H_{m,i} = 0$ and $D_{m,i} \neq 0$. The membrane free energy is minimized with respect to the shape and lateral and orientational distributions of membrane constituents. For small values of the intrinsic curvature deviator $D_{m,i}$, the tubular shape was proved energetically the most favorable. With increasing $D_{m,i}$, a certain critical value of $D_{m,i}$ is reached where the tubular shape is changed discontinuously to an undulated shape with a

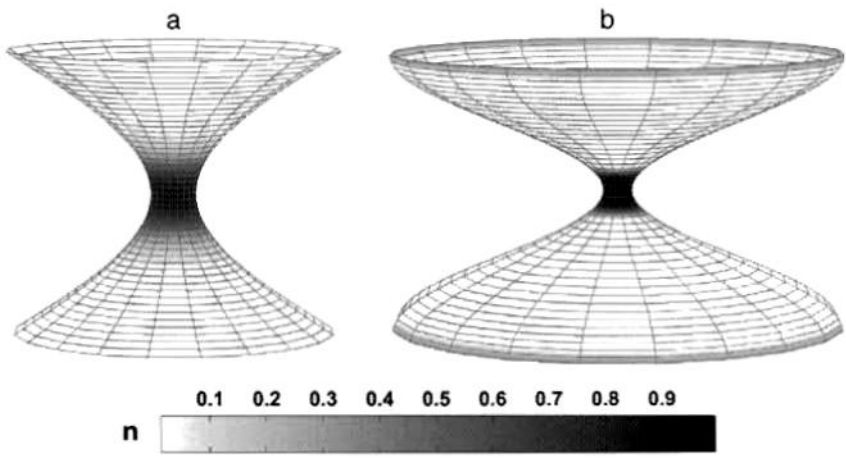


**Fig. 7.** The neck region of a membrane with anisotropic inclusions and the corresponding fraction of the membrane covered by inclusions (shaded); $H_{m,i} = H_{m,0} = 0$, $D_{m,0} = 0$, $D_{m,i} = 0.4\,\mathrm{nm}^{-1}$ (a) and $0.7\,\mathrm{nm}^{-1}$, (b) $\xi_i = \xi_j^* = 120kT\,\mathrm{nm}^2$, $\xi_0 = \xi_0^* = 12\,kT\,\mathrm{nm}^2$, $\bar{n} = 0.02$, $w = -0.1$, $l = 100\,\mathrm{nm}$ and $A = 2\pi \cdot 4000\,\mathrm{nm}^2$ (adapted from Ref. [21]).

narrow neck (Fig. 7). Figure 7 shows a part of the calculated membrane shape for two values of the intrinsic curvature deviator $D_{m,i}$ above the critical value ($D_{m,i,crit} \approx 0.33\,\mathrm{nm}^{-1}$). As can be seen in Fig. 7, the saddle-preferring anisotropic inclusions accumulate in the energetically favorable saddle-like neck regions. With increasing values of the intrinsic curvature deviator of anisotropic inclusions ($D_{m,i}$), the neck becomes thinner.

The results presented in Fig. 5 and in Fig. 7 indicate that two complementary mechanisms may take place in the budding of heterogeneous membranes containing isotropic and anisotropic constituents: accumulation of saddle-preferring membrane constituents in the neck connecting the bud and the parent membrane [21,23] and accumulation of strongly spherically curved membrane-preferring constituents in the spherical region of the bud (i.e. daughter vesicle) [5,13,17,42]. Figure 8 shows an increased fluorescence signal of cholera-toxin-labeled rafts on bursts of the membrane of the human urothelial line (RT4) cell. Clustering of rafts and membrane proteins in highly curved membrane regions (invaginations) and vesicles has also been previously observed [13,14,43].

In some cases the tendency for formation of a very long neck connecting the daughter vesicle and the mother membrane was observed [10,44–46]. Elongation of the neck connecting two compartments could be viewed as a possible physical mechanism of formation and stabilization of thin tubes that connect cells or cell organelles. These tubes might be important in transport of matter and information in cellular systems (Figs. 9 and 10). The results of some recent studies indicate that the vesicular transport between cell organelles over longer distances is not random and that it takes place between specific surface regions of the cell

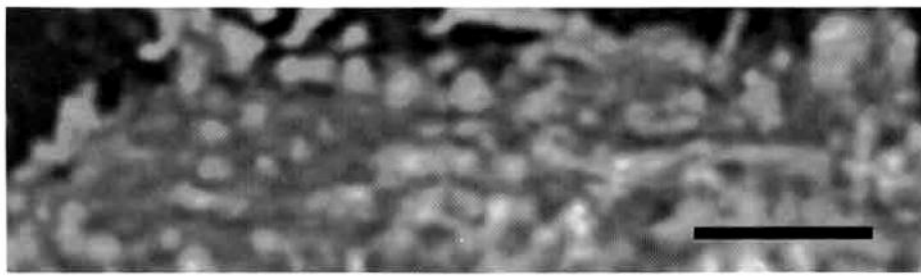

**Fig. 8.** A fluorescence microscope image of the budding membrane of human urothelial line RT4 cells. Differences in the intensity of the fluorescence signal indicate that cholera-toxin-labeled rafts accumulated on the buds. Bar = 200 nm (for color version: see Color Section on page 422).

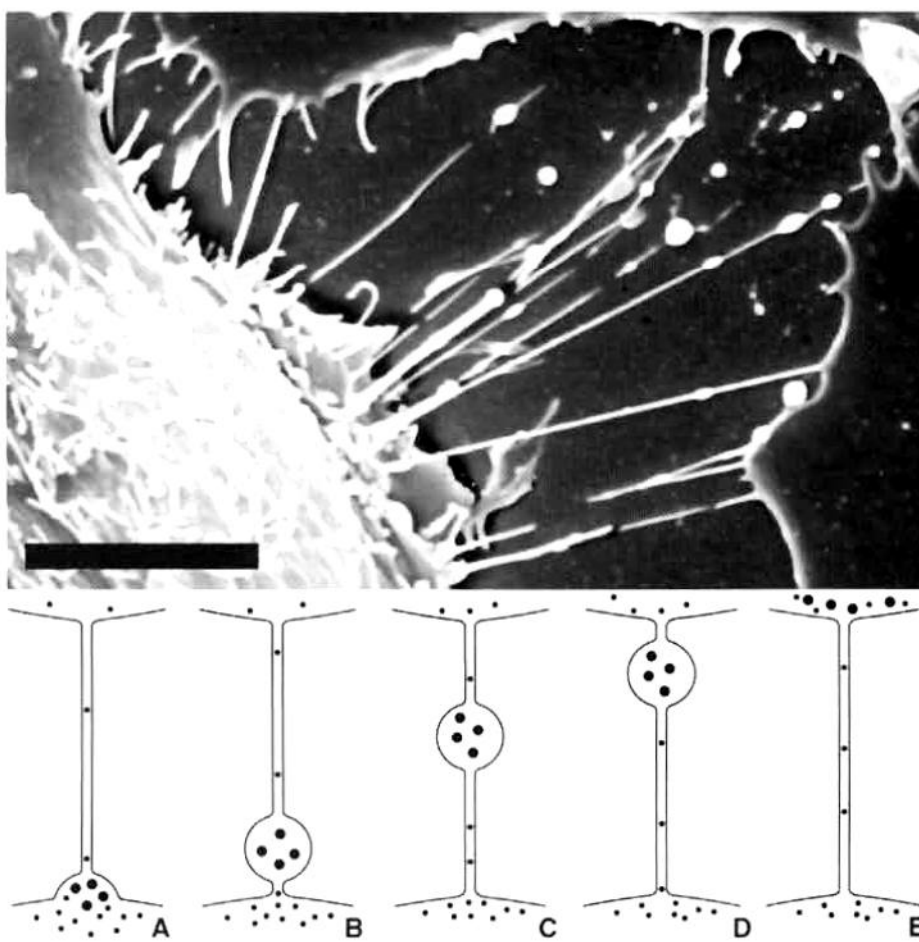


**Fig. 9.** Tubular structures with carrier vesicles as observed in cultures of human urothelial line RT4 cells (upper, bar = 10 μm), and the corresponding schematic illustration of nanotube-directed transport of carrier vesicles (A–D) and direct transport through nanotubes (E).

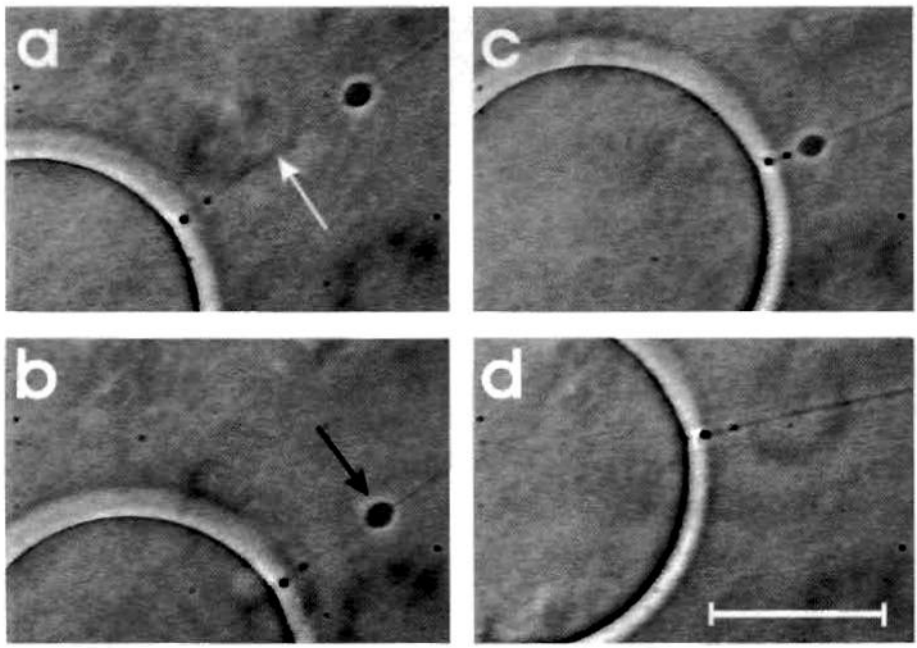


**Fig. 10.** Transport vesicles (black arrow) move along thin tubes in phospholipid vesicles. The transport vesicle is an integral part of the tube membrane. Bar = 10 μm (adapted from Ref. [48]).

organelles [42,47]. Such organized transport may be achieved by nanotube-directed transport of carrier vesicles or direct transport through nanotubes (Figs. 9 and 10) [48–51].

## 4. DETERGENT-INDUCED DOMAIN FORMATION AND ERYTHROCYTE SHAPE

It was observed that addition of detergents to the suspension of erythrocytes causes changes in the shape of erythrocyte. While the detergent molecules intercalate into the membrane, undulations of the membrane appear. Outward bending of the membrane leads to formation of echinocyte shape (Fig. 11), while inward bending of the membrane leads to formation of stomatocyte shape (Fig. 12), and further, to microvesiculation of the membrane [52–55]. Echinocytosis/stomatocytosis is determined by the species of intercalated detergent molecules. For example, dodecaylmaltoside, dodecylzwittergent and dioctyl-di-QAS induce echinocytosis and exovesiculation while chlorpromazine and ethyleneglycol-ethers induce stomatocytosis and endovesiculation [52]. The spherical/tubular/torocytic shape of the released vesicles is connected to the intrinsic shape of inclusions generated by the intercalated detergent molecules [54] and has been previously elaborated in detail [31]. Here, we point to the experimental evidence

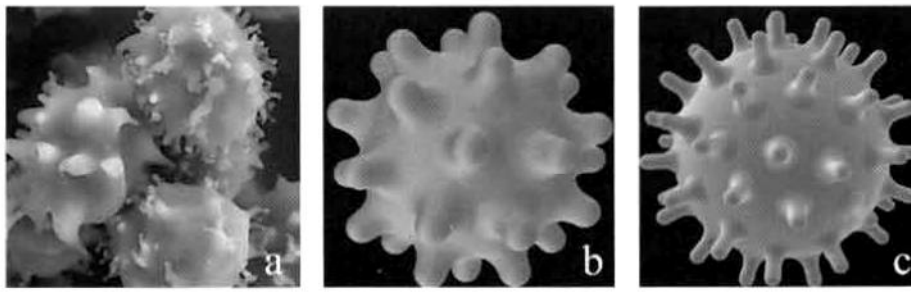


**Fig. 11.** A micrograph of echinocytes (adapted from Ref. [13]) (a) and the calculated echinocyte shapes determined by minimization of membrane elastic energy (bending and shear) for two different choices of environment parameters and relative cell volume 0.6 (b, c) (adapted from Refs. [53,55,65]).

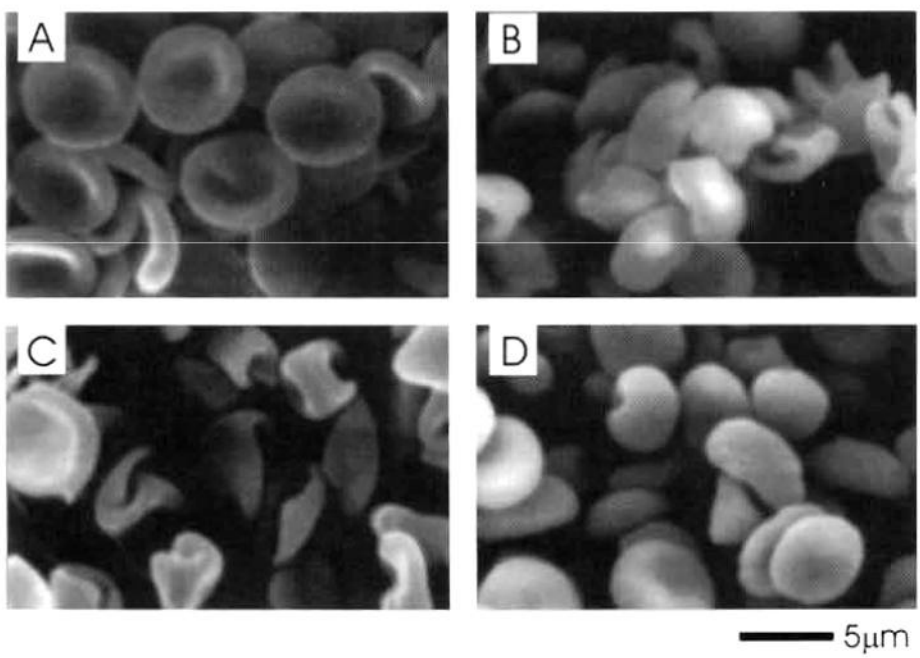


**Fig. 12.** Transformation of erythrocytes' shape 0 min (A), 5 min (B), 15 min (C) and 30 min (D) after addition of octaethyleneglycoldodecylther ($C_{12}E_8$) to the erythrocyte suspension. Erythrocytes first undergo a discocyte–stomatocyte transformation where the central invagination attains a flattened and sometimes twisted shape (B, C). Later, the mother cell becomes spherical while a peculiar-shaped endovesicles called torocytes appear inside the cell (adapted from Ref. [54]).

on the coexistence of lateral lipid domains in erythrocyte membrane, characterized by different order parameters and rotational correlation times [8,56] studied by using the ESR technique. Different detergents of the ethyleneglycol type $C_mE_n$ were added to the suspension containing erythrocytes (Fig. 13) and allowed to

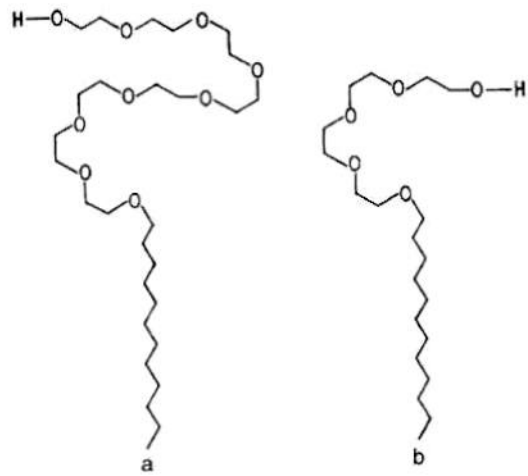


**Fig. 13.** Schematic illustrations of the chemical structure of octaethyleneglycol dodecyl;ether ($C_{12}E_8$) (A) and of tetraethyleneglycol dodecylether ($C_{12}E_4$) (B).

interact with the erythrocyte membrane [9]. It is expected that the hydrophobic tail of $C_mE_n$ incorporates into the hydrophobic portion of the membrane bilayer. The $C_{12}E_8$ molecule can be distinguished from the analogous $C_{12}E_4$ molecule as it has a larger hydrophilic head [57] (Fig. 13). The experimental ESR spectra of the control erythrocytes, as well as the spectra of $C_mE_n$ treated erythrocyte samples have been decomposed into three domain types, where the type I pertains to the most disordered fluid domain, and type III to the most ordered domain. The population proportions of the membrane domains, i.e. the relative weight factors are given in Fig. 14. They have been evaluated using the program EPR SIM 4.0 [56], by which the experimental spectra have been fitted with the calculated spectra for the considered domains.

The spin probe MeFASL(10,3) [58] (which is thought to distribute evenly between the inner and the outer leaflet) may report about the effects of the $C_mE_n$ molecules on the lateral domain distribution (domains I, II and III) at the level of the incorporated nitroxide. Figure 14 shows that $C_{12}E_4$ considerably changes the proportions of the membrane lipid domains relative to the control membrane, while $C_{12}E_8$ induces much smaller changes in the proportions of the domains. This may be partially due to the larger hydrophilic polyethylene head group of the $C_{12}E_8$ molecule that may not be pulled so deep into the membrane as the head group of the $C_{12}E_4$ molecule. Therefore the bound $C_{12}E_8$ induces a different perturbation at the level of the incorporated nitroxide than $C_{12}E_4$.

The above experimental evidence indicates that detergents change domain proportions and at the same time induce invagination and endovesiculation in erythrocyte membrane.

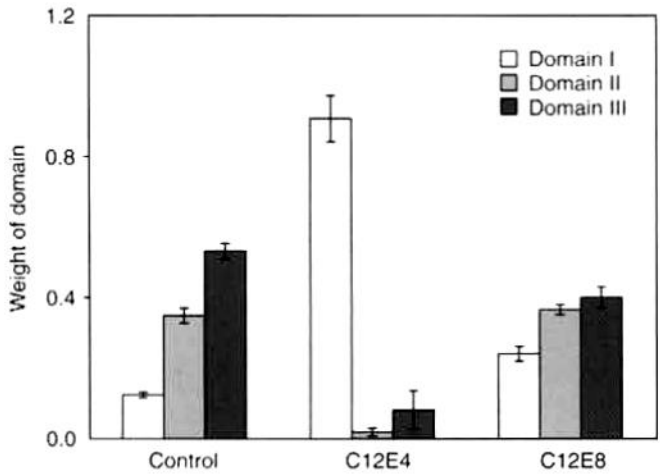


**Fig. 14.** The lateral domain population of the erythrocyte membrane for the control and $C_mE_n$-treated samples. The spin probe methyl ester of 5 dioxyl palmitate MeFASL(10,3) was used for EPR measurement. The bars indicate the standard deviations, referring to 5 independent experiments (adapted from Ref. [9]).

## 5. DISCUSSION

The coupling between the formation of raft domains and local anisotropic membrane curvature has been recently indicated in Golgi apparatus [42,47], where some of the membrane components are concentrated mainly on the bulbous rims of the Golgi cisternae, where the curvature deviator $D$ is very high. Similar phenomena have been suggested also in the photoreceptor discs [59,60] and flattened endovesicles of erythrocyte membrane [57] indicating that the coupling between the non-homogeneous lateral distribution of the membrane rafts and the specific membrane shapes may be a general mechanism of stabilization of highly curved membrane structures (flattened disc-like vesicles, spherical buds, necks, tubular protrusions) and membrane budding process and vesiculation [5,13,16,21,32,47]. The curvature-induced segregation and enrichment of membrane components in membrane protrusions have been discussed several times already in the past ([61] and references therein). However, all these studies were limited to short (spheroidal) membrane protrusions (buds) such as caveolae [13,62] or clathrin-coated buds [63]. In the present work we point to the influence of the anisotropy of the intrinsic shape of the membrane inclusions (described by intrinsic mean curvature $H_m$ and intrinsic curvature deviator $D_m$) on accumulation of inclusions also in other (non-spherical) shapes.

The predicted membrane shape changes due to the presence of membrane inclusions with high curvature deviator $D_m$ [22] can among other factors be applied to better explain the echinocyte membrane shape changes arising from conformational changes of membrane proteins induced by ligand binding or variation of ionic strength and pH [64]. Namely, the stable echinocyte shapes were

previously determined by minimization of membrane bilayer energy consisting of the bilayer bending energy, and shear and stretching energies of the membrane skeleton [65,66]. We suggest that the echinocyte shape may be additionally modulated by nonhomogeneous lateral distribution of membrane components [13].

In the above-described theoretical consideration of the membrane budding, we assumed that buds and released daughter vesicles are depleted of membrane skeleton. The presence of the membrane skeleton in the budding region would decrease the lateral mobility of the membrane constituents and thereby their ability to sort due to membrane curvature and/or direct interactions. In addition, the in-plane shear energy of the membrane skeleton would increase during the budding process [67] and the calculated shapes of membrane buds would be different from those presented in Fig. 5, especially in the vicinity of the neck region [68].

The clustering of the membrane inclusions (raft elements) into rafts and raft domains is promoted by direct interactions between the membrane inclusions [2]. The short-range phospholipid (and cholesterol) mediated attractive interactions between membrane inclusions [69] may offer a possible explanation for the nature of such interactions. Here, direct interactions between the anisotropic membrane constituents (inclusions) are considered within the Bragg–Williams approximation. Alternatively, they can be described by minimization of the boundary (line) tension between membrane domains [26]. However, considering the line tension assumes that the composition of the membrane domains is fixed in advance which is not in accordance with some experimental observation [14] and does not describe the process of formation of membrane domains where the composition may be gradually changed. The nearest-neighbor interaction term may cause the lateral phase separation (for $w<0$) also in the flat parts of the membrane if $|w|$ is large enough.

## ACKNOWLEDGMENT

Authors are grateful to A. Iglič, H. Hägerstrand and M. Bobrowska-Hägerstrand for discussions and support and B. Babnik and M. Fošnarič for assistance in preparing the figures.

## REFERENCES

[1] S.J. Singer, G.L. Nicholson, The fluid mosaic model of the structure of cell membranes, Science 175 (1972) 720–731.
[2] K. Jacobson, C. Dietrich, Looking at lipid raft? Trends Cell Biol. 9 (1999) 87–91.
[3] K. Simons, E. Ikonen, Functional rafts in cell membranes, Nature 387 (1997) 569–572.
[4] D.A. Brown, E. London, Structure and origin of ordered lipid domains in biological membranes, J. Membr. Biol. 164 (1998) 103–114.

[5] J.C. Holthius, G. van Meer, K. Huitema, Lipid microdomains, lipid translocation and the organization of intracellular membrane transport (review), Mol. Membr. Biol. 20 (2003) 231–241.
[6] D.M. Engelman, Membranes are more mosaic than fluid, Nature 438 (2005) 578–580.
[7] A. Weigmann, D. Corbeil, A. Hellwig, W.B. Huttner, Prominin, a novel microvilli-specific polytopic membrane protein of the apical surface of epithelial cells, is targeted to plasmalemmal protrusions of non-epithelial cells, Proc. Natl. Acad. Sci. USA 94 (1997) 12425–12430.
[8] M. Žuvić-Butorac, P. Müller, T. Pomorski, J. Libera, A. Herrmann, M. Schara, Lipid domain in the exoplasmic and cytoplasmic leaflet of the human erythrocyte membrane: a spin label approach, Eur. Biophys. J. 28 (1999) 302–310.
[9] M. Fošnarič, M. Nemec, V. Kralj-Iglič, H. Hägerstrand, M. Schara, A. Iglič, Possible role of anisotropic membrane inclusions in stability of torocyte red blood cell daughter vesicles, Coll. Surf. B 26 (2002) 243–253.
[10] W.B. Huttner, J. Zimmerberg, Implications of lipid microdomains for membrane curvature, budddng and fission, Curr. Opin. Cell Biol. 13 (2001) 478–484.
[11] G. Staneva, M. Seigneuret, K. Koumanov, G. Trugnan, M.I. Angelova, Detergents induce raft-like domains budding and fission from giant unilamellar heterogeneous vesicles. A direct microscopy observation, Chem. Phys. Lipids 136 (2005) 55–66.
[12] H.T. McMahon, J.L. Gallop, Membrane curvature and mechanisms of dynamic cell membrane remodelling, Nature 438 (2005) 590–596.
[13] H. Hägerstrand, L. Mrowczynska, U. Salzer, R. Prohaska, K.A. Michelsen, V. Kralj-Iglič, A. Iglič, Curvature dependent lateral distribution of raft markers in the human erythrocyte membrane, Mol. Membr. Biol. 23 (2006) 277–288.
[14] H. Hägerstrand, B. Isomaa, Lipid and protein composition of exovesicles released from human erythrocytes following treatment with amphiphiles, Biochim. Biophys. Acta 1190 (1994) 409–415.
[15] E. Sackmann, Membrane bending energy concept of vesicle and cell shapes and shape transitions, FEBS Lett. 346 (1994) 3–16.
[16] C. Thiele, M.J. Hannah, F. Fahrenholz, W.B. Huttner, Cholesterol binds to synaptophysin and is required for biogenesis of synaptic vesicles, Nat. Cell Biol. 2 (1999) 42–49.
[17] J.M. Holopainen, M.I. Angelova, P.K.J. Kinnunen, Vectorial budding of vesicles by asymmetric enzymatic formation of ceramide in giant liposomes, Biophys. J. 78 (2000) 830–838.
[18] M. Laradji, P.B.S. Kumar, Dynamics of domain growth in self-assembled fluid vesicles. Phys. Rev. Lett. 93 (2004) 198105/1–198105/4.
[19] M.M. Hanczyc, J.W. Szostak, Replicating vesicles as models of primitive cell growth and division, Curr. Opin. Chem. Biol. 8 (2004) 660–664.
[20] Y. Yamashita, S.M. Masum, T. Tanaka, Y. Tamba, M. Yamazaki, Shape changes of giant unilamellar vesicles of phosphatidiylcholine induced by a *de novo* designed peptide interacting with their membrane interface, Langmuir 18 (2002) 9638–9641.
[21] A. Iglič, B. Babnik, K. Bohinc, M. Fošnarič, H. Hägerstrand, V. Kralj-Iglič, On the role of anisotropy of membrane constituents in formation of a membrane neck during budding of a multicomponent membrane, J. Biomech. (2006) in print.
[22] V. Kralj-Iglič, H. Hägerstrand, P. Veranič, K. Jezernik, A. Iglič, Amphiphile-induced tubular buding of the bilayer membrane, Eur. Biophys. J. 34 (2005) 1066–1070.
[23] V. Kralj-Iglič, V. Heinrich, S. Svetina, B. Žekš, Free energy of closed membrane with anisotropic inclusions, Eur. Phys. J. B 10 (1999) 5–8.

[24] T. Shemesh, A. Luini, V. Malhotra, K.N.J. Burger, M.M. Kozlov, Prefission constriction of Golgi tubular carriers driven by local lipid metabolism: a theoretical model, Biophys. J. 85 (2003) 3813–3827.
[25] W. Wiese, W. Harbich, W. Helfrich, Budding of lipid bilayer vesicles and flat membranes, J. Phys. Consdens. Matter 4 (1992) 1647–1657.
[26] R. Lipowsky, Budding of membranes induced by intramembrane domains, J. Phys. II (France) 2 (1992) 1825–1840.
[27] A. Iglič, H. Hägerstrand, Amphiphile-indiced spherical microexovesicles correponds to an extreme local area difference between two monolayers of the membrane bilayer, Med. Biol. Eng. Comput. 37 (1999) 125–129.
[28] V. Kralj-Iglič, S. Svetina, B. Žekš, Shapes of bilayer vesicles with membrane embedded molecules. Eur. Biophys. J. 24 (1996) 311–321.
[29] L.B. Fournier, Nontopological saddle-splay and curvatur instabilities from anisotropic membrane inclusions, Phys. Rev. Lett. 76 (1996) 4436–4439.
[30] V. Kralj-Iglič, A. Iglič, G. Gomišček, V. Arrigler, H. Hägerstrand, Microtubes and nanotubes of phospholipid bilayer vesicles, J. Phys. A: Math. Gen. 35 (2002) 1533–1549.
[31] A. Iglič, V. Kralj-Iglič, Effect of anisotropic properties of membrane constituents on stable shape of membrane bilayer structure, in: H. Ti Tien, A. Ottova-Leitmannova (Eds.), Planar Lipid Bilayers (BLMs) and their Applications, Elsevier, Amsterdam, London, 2003, pp. 143–172.
[32] A. Iglič, H. Hägerstrand, P. Veranič, A. Plemenitaš, V. Kralj-Iglič, Curvature-induced accumulation of anisotropic membrane components and raft formation in cylindrical membrane protrusions, J. Theor. Biol. 240 (2006) 368–373.
[33] T.L. Hill, An Introduction to Statistical Thermodynamics, General Publishing Company, Toronto, 1986, pp. 209–211.
[34] V.S. Markin, Lateral organization of membranes and cell shape, Biophys. J. 36 (1981) 1–19.
[35] L. Miao, B. Fourcade, M. Rao, M. Wortis, R.K.P. Zia, Equilibrium budding and vesiculation in the curvature model of fluid lipid vesicles, Phys. Rev. E 43 (1991) 6843–6856.
[36] L. Miao, U. Seifert, M. Wortis, H.G. Döbereiner, Budding transitions of fluid-bilayer vesicles: effect of area difference elasticity, Phys. Rev. E 49 (1994) 5389–5407.
[37] I. Derényi, F. Jülicher, J. Prost, Formation and interaction of membrane tubes, Phys. Rev. Lett. 88 (2002) 238101/1–238101/4.
[38] K. Röper, D. Corbeil, W.B. Huttner, Retention of prominin in microvilli reveals distinct cholesterol-based lipid microdomains in the apical plasma membrane, Nat. Cell Biol. 2 (2000) 582–592.
[39] M. Fosnarič, K. Bohinc, D.R. Gauger, A. Iglič, V. Kralj-Iglič, S. May, The influence of anisotropic membrane inclusions on curvature elastic properties of lipid membranes, J. Chem. Inf. Model. 45 (2005) 1652–1661.
[40] A.A. Boulbitch, Deflection of a cell membrane under application of local force, Phys. Rev. E 57 (1998) 1–5.
[41] V. Kralj-Iglič, A. Iglič, H. Hägerstrand, P. Peterlin, Stable tubular microexovesicles of the erythrocyte membrane induced by dimeric amphiphiles, Phys. Rev. E 61 (2000) 4230–4234.
[42] H. Sprong, P. van der Sluijs, G. van Meer, How proteins move lipids and lipids move proteins, Nat. Cell Biol. 2 (2001) 504–513.
[43] T. Harder, K. Simons, Caveolae, DIGs, and the dynmics of sphingolipid–cholesterol microdomains, Curr. Opin. Cell Biol. 9 (1997) 534–542.
[44] H. Gad, P. Löw, E. Zotova, L. Brodin, O. Shupliakov, Dissociation between $Ca^{2+}$-triggered synaptic vesicle exocytosis and clathrin-mediated endocytosis at a central synapse, Neuron 21 (1998) 607–616.

[45] V. Kralj-Iglič, A. Iglič, M. Bobrowska-Hägerstrand, H. Hägerstrand, Tethers connecting daughter vesicles and parent red blood cell may be formed due to ordering of anisotropic membrane constituents, Coll. Surf. A 179 (2001) 57–64.
[46] L. Rajendran, M. Masilamani, S. Solomon, R. Tikkanen, C.A. Stuermer, H. Plattner, H. Illges, Asymmetric localization of flotillins/reggies in preaseembled platforms confers inherent polarity to hematopoietic cells, Proc. Natl. Acad. Sci. (USA) 100 (2003) 8241–8246.
[47] A. Iglič, M. Fošnarič, H. Hägerstrand, V. Kralj-Iglič, Coupling between vesicle shape and the non-homogeneous lateral distribution of membrane constituents in Golgi bodies, FEBS Lett. 574 (1–3) (2004) 9–12.
[48] A. Iglič, H. Hägerstrand, M. Bobrowska-Hägerstrand, V. Arrigler, V. Kralj-Iglič, Possible role of phospholipid nanotubes in direct transport of membrane vesicles, Phys. Lett. A 310 (2003) 493–497.
[49] M. Elsner, H. Hashimoto, T. Nilsson, Cisternal maturation and vesicle transport: join the band wagon, Mol. Membr. Biol. 20 (2003) 221–229.
[50] A. Rustom, R. Saffrich, I. Marković, P. Walther, H.H. Gerdes, Nanotubular highways for intracellular organelle transport, Science 303 (2004) 1007–1010.
[51] M. Sun, J.S. Graham, B. Hegedüs, F. Marga, Y. Zhang, G. Forgacs, Multiple membrane tethers by atomic force microscopy, Biophys. J. 89 (2005) 4320–4329.
[52] H. Hägerstrand, B. Isomaa, Morphological characterization of exovesicles and endovesicles released in human erythrocytes following treatment with amphiphiles, Biochim. Biophys. Acta 1109 (1992) 117–126.
[53] A. Iglič, V. Kralj-Iglič, H. Hägerstrand, Amphiphile induced echinocyte–spheroechinocyte transformation of red blood cell shape, Eur. Biophys. J. 27 (1998) 335–339.
[54] M. Bobrowska-Hägerstrand, V. Kralj-Iglič, A. Iglič, K. Bialkowska K, B. Isomaa, H. Hägerstrand, Torocyte membrane endovesicles induced by octaethyleneglycol dodecylether in human erythrocytes, Biophys. J. 77 (1999) 3356–3362.
[55] A. Iglič, P. Veranič, K. Jezernik, M. Fošnarič, V. Kralj-Iglič, H. Hägerstrand, Spherocyte shape transformation and release of tubular nanovesicles in human erythrocytes, Bioelectrochemistry 62 (2004) 159–161.
[56] M. Štrancar, M. Šentjurc, M. Schara, Fast and accurate characterization of biological membrane by EPR spectral simulations of nitroxides, J. Magn. Reson. 142 (2000) 254–265.
[57] H. Hägerstrand, V. Kralj-Iglič, M. Fošnarič, M. Bobrovska-Hägerstrand, L. Mrowczynska, T. Söderström, A. Iglič, Endovesicle formation and membrane perturbation induced by polyoxyethyleneglycolalkylethers in human erythrocytes, Biochim. Biophys. Acta 1665 (2004) 191–200.
[58] J. Svetek, B. Kirn, B. Vilhar, M. Schara, Lateral domain diversity in membranes of callus and root cells of potato as revealed by EPR spectroscopy, Physiol. Plant 105 (1999) 499–505.
[59] R.S. Molday, D. Hicks, L. Molday, Peripherin. A rim specific membrane protein of rod outer segment discs, Invest. Ophthalmol. Vis. Sci. 28 (1987) 50–61.
[60] D. Corbeil, K. Röper, C.A. Fargeas, A. Joester, H.B. Huttner, H.B., Prominin: a story of cholesterol, plasma membrane protrusions and human pathology, Traffic 2 (2001) 82–91.
[61] P.B.S. Kumar, G. Gompper, R. Lipowsky, Budding dynamics of multicomponent membranes, Phys. Rev. Lett. 86 (2001) 3911–3914.
[62] P. Sens, M.S. Turner, Theoretical model for the formation of caveolae and similar membrane invaginations, Biophys. J. 86 (2004) 2049–2057.
[63] J.B. Fournier, P.G. Dommersnes, P. Galatola, Dynamin recruitment by clathrin coats: physical step? C.R. Biol. 326 (2003) 467–476.
[64] J. Gimsa, C. Ried, Do band 3 protein conformation changes mediate shape changes of human erythrocyte? Mol. Membr. Biol. 12 (1995) 247–254.

[65] A. Iglič, A possible mechanism determining of stability of spiculated red blood cells, J. Biomech. 30 (1997) 35–40.
[66] R. Mukhopadhyay, G. Lim, M. Wortis, Echinocyte shapes: bending, stretching and shear determine spicule shape and spacing, Biophys. J. 82 (2002) 1756–1772.
[67] H. Hägerstrand, V. Kralj-Iglič, M. Bobrowska-Hägerstrand, A. Iglič, Membrane skeleton detachment in spherical and cylindrical microexovesicles, Bull. Math. Biol. 61 (1999) 1019–1030.
[68] T. Kosawada, K. Inoue, G.W. Schmid-Schönbein, Mechanics of curved plasma membrane vesicles: resting shapes, membrane curvature, and in-plane shear elasticity, ASME J. Biomech. Eng. 127 (2005) 229–236.
[69] K. Bohinc, V. Kralj-Iglič, S. May, Interaction between two cylindrical inclusions in a symmetric lipid bilayer, J. Chem. Phys. 119 (2003) 7435–7444.